


**Please cite the Published Version**

Li, Z, Meng, Z, Haigh, A, Wang, P and Gibson, A  (2021) Characterisation of water in honey using a microwave cylindrical cavity resonator sensor. Journal of Food Engineering, 292. p. 110373. ISSN 0260-8774

**DOI:** <https://doi.org/10.1016/j.jfoodeng.2020.110373>

**Publisher:** Elsevier

**Version:** Accepted Version

**Downloaded from:** <https://e-space.mmu.ac.uk/627748/>

**Usage rights:**  In Copyright

**Additional Information:** This is an Author Accepted Manuscript of an article published in Journal of Food Engineering by Elsevier.

**Enquiries:**

If you have questions about this document, contact [openresearch@mmu.ac.uk](mailto:openresearch@mmu.ac.uk). Please include the URL of the record in e-space. If you believe that your, or a third party's rights have been compromised through this document please see our Take Down policy (available from <https://www.mmu.ac.uk/library/using-the-library/policies-and-guidelines>)

Characterisation of water in honey using a microwave cylindrical cavity resonator sensor

Zhen Li<sup>1\*</sup>, Zhaozong Meng<sup>2</sup>, Arthur Haigh<sup>3</sup>, Ping Wang<sup>1</sup>, and Andrew Gibson<sup>4</sup>

<sup>1</sup>College of Automation Engineering, Nanjing University of Aeronautics and Astronautics,

Nanjing, 211106, China

<sup>2</sup>School of Mechanical Engineering, Hebei University of Technology, Tianjin 300130, China

<sup>3</sup>Department of Electrical and Electronic Engineering, The University of Manchester,

Manchester, M13 9PL, UK

<sup>4</sup>Faculty of Science and Engineering, Manchester Metropolitan University,

Manchester, M1 5GD, UK

\*Corresponding author: [zhenli@nuaa.edu.cn](mailto:zhenli@nuaa.edu.cn)

## **Abstract**

A low-cost microwave cavity resonator sensor is developed for the assessment of honey. When a liquid sample is placed in the cavity, the resonant responses are significantly changed caused by the material perturbation. From the measurement of standard liquid samples with known permittivity, it is demonstrated that the electric permittivity can be accurately determined. For the honey-water mixtures with the added water content from 10% to 50% w/w, it is found that the resonance frequency decreases with increasing added water content, and its change conforms to the law of mixture. In addition, there is a linear relationship between the added water content and the real part of the effective permittivity, and a quadratic relationship is found between the real and imaginary parts of the permittivity. These findings agree well with the results of the mixtures with an added water content below 10%. Hence, both the resonant responses of the cavity and the permittivity obtained can be employed for the indication of adulteration and accurate evaluation of the water content. Further, it is shown that full penetration of the liquid sample can be achieved. The microwave sensor presented here provides an alternative tool for rapid food evaluation.

Keywords: honey adulteration; water content; cavity resonator; permittivity

## 1 Introduction

As a pure product, honey has been used as both a highly nutritious food and a medicine for some diseases. It should be free from addition of any other substance, which includes but is not limited to water or other sweeteners (Zábrodská & Vorlová, 2014). However, due to economic gain, adulteration of honey has been on the rise in recent years. A number of methods have been proposed for the detection, such as sensory and chemical analyses. The sensory analysis is readily performed, where the panellists assess the colour, viscosity, smell, flavour and crystallisation of the honey under test. However, the accuracy provided is strongly dependent on the panellists' experience. By comparison, the chemical methods (e.g., liquid chromatography (Wang et al., 2015), near infrared spectroscopy (Bázár et al., 2016; L. Chen et al., 2011) and mass spectrometry (Blasco, Fernández, Picó, & Font, 2004; Hammel, Mohamed, Gremaud, LeBreton, & Guy, 2008)) are more accurate, while expensive equipment and trained personnel are highly demanded. Hence, the search for an economical and easy-to-use sensor is of great necessity.

The microwave-based techniques can be introduced as alternative methods for food analysis (Blakey & Morales-Partera, 2016; Gibson et al., 2008). Microwave methods have various advantages, such as fast (few minutes rather than hours), low cost, low signal power (up to few milliWatts), good reproducibility and no hazards. In this type of approach, the electric permittivity ( $\epsilon_r = \epsilon'_r - j\epsilon''_r$ ), an intrinsic material property that describes the interaction with the electromagnetic field applied, is the parameter of interest. The real part  $\epsilon'_r$  (also called dielectric constant) characterises the ability of a material to store the electric field energy, and the imaginary part  $\epsilon''_r$  (also called dielectric loss factor) indicates the energy absorption. Over the microwave range, the dipole rotation and ionic conduction are the dominant loss mechanisms.

The permittivity measurement methods can be categorised into non-resonant methods (e.g., transmission line techniques, open-ended methods and free space measurements) and resonant methods (Krupka, 2006). Generally, a wideband permittivity can be provided by non-resonant methods, while the accuracy of the loss factor measurement is limited. In comparison, the resonant approach is inherently narrowband, and resonators (e.g., cavities and open resonators) need to be constructed instead of using the commercially available microwave components like waveguides and antennas in the non-resonant methods. However, the highest possible accuracy can be achieved. In addition, in terms of the sample preparation, a smaller sample volume is required. For honey, Puranik et al. (Puranik, Kumbharkhane, & Mehrotra, 1991) investigated the dielectric properties of honey-water mixtures using the time-domain technique in the frequency range of 10 MHz-10 GHz. The setup consisted of a time domain reflectometer unit, a pulse generator, an oscilloscope, coaxial

cables and a personal computer. Measures were taken to ensure that the incident signal was separated from the pulse reflected. Appropriate signal processing involving time shifting and Fourier transform was used to convert the time-domain signals to the frequency-domain for permittivity determination. The Davidson-Cole relaxation distribution was introduced to fit the permittivity spectrum, and the dielectric parameters associated (e.g., static dielectric constant and relaxation time) were extracted. The variations of the parameters with respect to the water content were presented. Guo et al. (Guo, Zhu, Liu, & Zhuang, 2010) measured the permittivity of the water-adulterated honey with a water content from 18% to 42.6% over 10 MHz-4.5 GHz. The dielectric constant of the mixture decreased monotonically with increasing frequency and increased with a higher water content. In the test, a commercial open-ended probe was used, and the probe tip was immersed in the liquid under test. Li et al. (Li, Haigh, Soutis, Gibson, & Sloan, 2017) employed the transmission line method for permittivity calculation of honeys. Over 6-8 GHz, it was also found that the effective permittivity of the honey-water mixture increased with more water added. Linear and quadratic relationships were revealed between the permittivity and the added water content. In the test setup, the honey was positioned in a hollow rectangular waveguide cell and between two Perspex windows. The data collection process was conducted right after the liquid placement to avoid liquid leakage. Hence, careful implementation was required. Gennarelli et al. (Gennarelli, Romeo, Scarfi, & Soldovieri, 2013) designed a rectangular cavity resonator for concentration measurements of water/NaCl and water/sucrose solutions. Calibration curves were obtained using the data of the transmission coefficient at the peak and the resonance frequency shift. However, no details about the permittivity of the solutions were provided. Furthermore, the discussion of the applicability of the resonant cavity for the evaluation of honey is not found in the literature.

Here, a microwave resonant approach using a cylindrical cavity resonator is proposed for the measurement of honey for the first time. First, the design of the sensor is presented. The permittivity calculation procedure using the perturbation technique is described for the sample positioning adopted. Then electromagnetic simulation is performed to investigate the field distributions at resonance. The measurement results of standard liquids with known permittivity values are compared with the reference data to check the accuracy of the test system. The permittivity of honey and honey-water mixtures is evaluated, and the effect of the water content on the resonant responses is discussed in detail. The sensor performance in terms of signal penetration is examined whether volumetric measurement can be performed.

## 2 Materials and methods

### 2.1 Standard liquids and honey samples

Four standard liquids with known permittivity values were used for the assessment of the measurement accuracy, i.e., distilled water, ethanol ( $\geq 99.8\%$  purity), isopropyl alcohol (IPA) ( $\geq 99.7\%$  purity) and 0.1 M NaCl solution (the purity of sodium chloride used was at least 99.8%). In the preparation of the solution, the mass of sodium chloride was accurately measured by an electronic balance (HC<sup>®</sup>) with a precision of 0.001 g. The solution was thoroughly mixed using a volumetric flask.

A bottle of Acacia honey was purchased from a local supermarket. It contains 2.5 g of fat, 79.8 g of carbohydrates and 25 mg of salt per 100 g. The effect of added water on the permittivity of honey was studied with different added water amounts (i.e., 10%, 20%, 30%, 40% and 50%, w/w). A maximum added water content  $\zeta$  of 50 % was adopted, as with more water added the mixture turned less viscous and more readily detected by visual inspection. Water was added to honey in a 25 mL glass beaker and the mixture was slowly stirred with a glass stick for thorough mixing. Then, the sample was placed within a quartz tube, which was inserted into the resonant cavity.

### 2.2 Cavity resonator design

The cavity resonator was made of aluminium, and the fabrication cost was around US\$ 60. The diagram of the structure is illustrated in Figure 1. It has a cylindrical wall and two endplates and socket screws are used to tightly join the components. External power is fed into the cavity with a small wire probe, which is made by extending the inner conductor of a SMA (SubMiniature version A) connector. The current in the short probe is small, but the voltage creates an electric field between the probe and the endplate, inducing signal excitation. A second wire probe is used to sense the field magnitude. A hole is drilled at the centre of each endplate, where a liquid-filled fused quartz tube can be inserted for measurement. The dimensions of the cavity and tube are listed in Table 1.

Figure 1 Schematic diagram of the cylindrical cavity resonator: (a) cavity; (b) quartz tube with liquid

Table 1 Dimensions of the cavity resonator sensor and quartz tube

Radius of the cavity $a$	Height of the cavity $h$	Inner radius of the tube $r_1$	Outer radius of the tube $r_2$
(mm)	(mm)	(mm)	(mm)
46.00	40.00	0.50	1.50

The cavity is operated in the  $TM_{010}$  mode, which is the dominant  $TM_{nml}$  mode. TM (transverse magnetic) means that the magnetic field is transverse to the propagation direction (i.e., the axis of the cylinder). The subscripts  $n$ ,  $m$  and  $l$  indicate the numbers of the half-sinusoid variations in the standing wave pattern along the circumferential, radial and axial directions, respectively. At this mode the resonance frequency can be given by (Pozar, 2012)

$$f_{TM_{010}} = \frac{cp_{01}}{2\pi a} \quad (1)$$

where  $c$  is the speed of light in free space,  $p_{01}=2.405$  is the 1<sup>st</sup> root of the Bessel function of first kind  $J_0$ , and  $a$  is the radius of the cavity. From Equation (1) it is implied that the operating frequency of the cavity is around 2.50 GHz. The real operating frequency may slightly change in different tests and causes a negligible difference. The frequency is close to 2.45 GHz, which is the commonly used frequency for microwave processing in both food industry and households (e.g., microwave ovens) (Regier, Knoerzer, & Schubert, 2017). Hence, the permittivity values obtained by the sensor can provide useful references for certain applications.

### 2.3 Permittivity calculation

The perturbation method is applied to extract the permittivity of liquid. It is assumed that with a small material perturbation (i.e., the liquid-filled quartz tube in the present case) the actual fields of a cavity are not significantly different from those of the original cavity. The resonance frequency change caused by the sample can be approximated by (Collin, 2000)

$$\frac{f_2 - f_1}{f_1} \approx \frac{-\int_{V_c} (\Delta\epsilon |\bar{E}_1|^2 + \Delta\mu |\bar{H}_1|^2) dv}{\int_{V_c} (\epsilon |\bar{E}_1|^2 + \mu |\bar{H}_1|^2) dv} \quad (2)$$

where  $f_1$  and  $f_2$  are the resonant frequencies before and after the perturbation, respectively.  $\epsilon$  and  $\mu$  are the electric permittivity and magnetic permeability of the material in the unperturbed cavity, respectively. Here the original cavity is air-filled, so  $\epsilon$  and  $\mu$  are close to two constants  $\epsilon_0$  and  $\mu_0$ , which are the permittivity and permeability of free space, respectively.  $|\bar{E}_1|$  and  $|\bar{H}_1|$  are the original electric and magnetic fields, respectively.  $V_c$  is the volume of the cavity.  $\Delta\epsilon$  and  $\Delta\mu$  are the changes of the permittivity and permeability in the cavity, respectively.

Taking the non-magnetic tube and liquid as a whole, for the cylindrical sample with a radius of  $r$  (i.e.,  $r_2$  in the present case) and a height of  $h$  placed in the centre of the cavity, the permittivity of the sample  $\epsilon_r$  can be resolved by substituting the expressions of the  $TM_{010}$  mode fields into Equation (2) (L. F. Chen, Ong, Neo, Varadan, & Varadan, 2004)

$$\varepsilon'_r \approx 1 + 2J_0'^2(p_{01}) \frac{a^2}{r^2} \frac{f_1 - f_2}{f_2} \quad (3a)$$

$$\varepsilon''_r \approx J_0'^2(p_{01}) \frac{a^2}{r^2} \left( \frac{1}{Q_2} - \frac{1}{Q_1} \right) \quad (3b)$$

where  $Q_1$  and  $Q_2$  are the quality factors before and after perturbation, respectively.  $J'_0$  is the derivative of  $J_0$  with respect to its argument, and  $J_0'^2(p_{01})$  is approximately 0.2696.

In Equation (3b) an unloaded quality factor (commonly denoted by  $Q_U$ ) should be used. It is a characteristic of the resonator itself without any loading effects caused by the external circuitry. However, due to the cavity coupling, the quality factor derived from the signal response is normally reduced, and it is often called the loaded quality factor  $Q_L$ .  $Q_L$  can be converted to  $Q_U$  to eliminate the effect of the coupling on the permittivity calculation (Pozar, 2012)

$$Q_U = (1 + g) Q_L \quad (4)$$

where  $g$  is the coupling coefficient and can be given by

$$g = \frac{S_{21}(f_1)}{1 - S_{21}(f_1)} \quad (5)$$

From the effective permittivity  $\varepsilon_r$  given by Equation (3), the permittivity of the liquid  $\varepsilon_{r1}$  can be extracted

$$\varepsilon_{r1} = \frac{\varepsilon_r - (1 - \xi) \varepsilon_{r2}}{\xi} \quad (6)$$

where  $\varepsilon_{r2}$  is the relative permittivity of the tube.  $\xi = r_1^2 / r_2^2$  is the cross-sectional area ratio of the liquid sample to the hole in the endplate.

## 2.4 Experimental setup

The schematic diagram of the experimental setup is illustrated in Figure 2. The sensor is connected to a portable N9951A Fieldfox microwave analyser (300 kHz-44 GHz) by two coaxial cables (A-info SM-SM-SFD147A, DC-18 GHz). The analyser has a frequency resolution of 1 Hz for an operating frequency below 5 GHz and a log magnitude resolution of 0.01 dB. The analyser is directly connected to a personal computer (PC) by a LAN cable. A MATLAB<sup>®</sup> programme is used for data acquisition.

In the test, the analyser was operated in the NA (network analyser) mode, and a frequency range of 2.4-2.5 GHz was used with 4001 sampling points. The signal power was set to -15 dBm (i.e., 0.032 mW) to minimise any potential heating effect. A low intermediate frequency bandwidth (IFBW) value, i.e., 100 Hz, was chosen to reduce the noise floor. A factory calibration known as CalReady



was adopted, where the calibration was performed at the port 1 and port 2 connectors. The calibration can correct measurements when the analyser is turned on and when a measurement is created with no other correction in place.

All the experiments were conducted at room temperature ( $25 \pm 1$  °C). Special care was taken to prevent any air bubbles from being trapped inside the liquid. In addition, the tube was placed at the same position and the volume of the liquid sample was made the same. Little liquid leakage was observed as the tube was in the horizontal plane.

Figure 2 Schematic diagram of the experimental setup for the evaluation of liquid with a microwave cylindrical cavity resonator sensor

### 3 Results and discussion

#### 3.1 Electromagnetic simulation

An electromagnetic model of the resonator is built in CST<sup>®</sup> simulation software. As shown in Figure 3 (a), the microwave signal is introduced at the top endplate with a waveguide port. The frequency domain solver is used with a frequency range of 2.4-2.5 GHz. The adaptive mesh refinement option in the solver setting is chosen to obtain a reasonable mesh resolution. Variation of the transmission coefficient  $S_{21}$  for the empty cavity is presented in Figure 3 (b), where the resonance frequency (i.e., 2.4942 GHz) is very close to the theoretical value. The field distributions at resonance are shown in Figure 4, where the magnetic field has only the azimuthal component as would be expected and the electric field has the dominant axial component with the maximum at the axis. Hence, it is indicated that the placement of the sample along the axis can better disturb the fields, achieving an optimal measurement sensitivity.

(a) (b)

Figure 3 Electromagnetic simulation of the cavity resonator: (a) cross section of the model; (b) resonant responses of the empty cavity

(a) (b)

Figure 4 Simulation results of the field distribution within the cavity at resonance: (a) electric field; (b) magnetic field

### 3.2 Measurement of the empty cavity and standard materials

(1) Empty cavity: In the present work the Lorentzian distribution function is employed for the calculation of the loaded quality factor  $Q_L$  and resonance frequency  $f_r$  from the transmission coefficient measurement by curve fitting. Near the resonance, the transmission power  $A$  can be approximated by

$$A(f) = \frac{A_p}{1 + 4Q_L^2 \left( \frac{f - f_r}{f_r} \right)^2} \quad (7)$$

where  $A = |S_{21}|^2$  is a function of the operating frequency  $f$ , and its maximum is represented by  $A_p$ . The two unknown parameters,  $Q_L$  and  $f_r$ , can be computed using the method of least squares. As shown in Figure 5, good agreement is obtained between the original data and the fitted response curve. For better presentation only the first out of every five raw data points is displayed. The resonance frequency and  $Q_U$  obtained from Equations (4) and (5) are listed in Table 2. It is seen that the resonant frequency is accurately predicted by the simulation with an error of 1 %. The quality factor of the real cavity is much lower than that by the simulation (approximately 12622) due to the marginal leakage at the joins between the endplates and the cylindrical wall.

(2) Standard samples: The resonant responses of the standard liquid samples are presented in Figure 6 and Table 2. Each sample was measured three times. In the repeated measurements, the resonance frequency is unchanged, while small variations are seen in the quality factor. All the quality factors are one order of magnitude lower than that of the empty cavity case, indicating the strong energy absorption by the samples.

For permittivity calculation,  $\epsilon_r$  of fused quartz at 25 °C and 2.50 GHz (i.e.,  $3.78 - j2.30 \times 10^{-4}$  (Hippel, 1995)) is used.  $\epsilon_r$  of the standard samples measured are listed in Table 3. Compared with the theoretical values found in the literature, the measurement errors are well within in  $\pm 5$  % (except  $\epsilon'_r$  of water where the error is slightly larger than 5 %). It is well demonstrated that the microwave sensor developed could provide high measurement accuracy that is comparable to that of a commercial dielectric probe ( $\pm 5$  % for both  $\Delta \epsilon'_r / |\epsilon_r|$  and  $\Delta \epsilon''_r / |\epsilon_r|$  (Agilent Technologies, 2006)).

Figure 5 Fitted Lorentzian curve for the empty cavity case

Figure 6 Signal responses of the cavity with standard liquid samples

Table 2 Resonant parameters of the empty cavity and standard liquids measured

	Empty cavity	Water	Ethanol	IPA	0.1M NaCl solution
Resonance frequency $f_r$ (GHz)	2.4917	2.4377	2.4765	2.4780	2.4390
Quality factor $Q_U$	2010.40±3.35	213.18±3.49	287.18±5.30	549.95±3.62	118.33±5.63

Table 3 Permittivity of standard samples given by the cavity resonator

	Water	Ethanol	IPA	0.1M NaCl solution
Reference data	76.90-j9.41 (Cole & Cole, 1941)	7.25-j6.98 (Gregory & Clarke, 2012)	4.00-j2.98 (Gregory & Clarke, 2012)	75.02-j16.11 (Stogryn, 1971)
Present work	80.98-j9.96(±0.19)	6.98-j7.09(±0.15)	4.12-j3.14(±0.03)	78.50-j18.90(±0.96)
Error averaged ( $\Delta\epsilon'_r/ \epsilon_r $ , %)	5.14	-2.68	2.41	4.54
Error averaged ( $\Delta\epsilon''_r/ \epsilon_r $ , %)	0.06	1.09	3.21	3.64

### 3.3 Permittivity of honey

The resonant responses of the honey sample is shown in Figure 7. The resonance frequency is shifted downwards to 2.4748 GHz. The quality factor (around 354.50) is higher than that of the water case, thereby indicating that the honey is not as lossy as water. The permittivity of the honey calculated is 10.13-j5.52, which agrees well with the quality factor analysis. And the result is comparable with the data of other types of honeys reported in the literature (Guo et al., 2010; Puranik et al., 1991).

Figure 7 Resonant responses of the honey sample

### 3.4 Permittivity of water-added honey

The resonant responses of the all the adulteration cases are shown in Figure 8 and Table 4. The test of the honey sample with no added water is taken as a reference. It is noticed that the resonance frequency is gradually reduced as  $\zeta$  increases. At  $\zeta=50$  %, the resonant frequency is still higher than that of the pure water case. The conventional law-of-mixture analysis technique is introduced to investigate the relationship between the added water content and resonant frequency of the mixture:

$$f_{rm} = \zeta f_{rw} + (1 - \zeta) f_{rh} \quad (8)$$

where  $f_{rm}$ ,  $f_{rw}$  and  $f_{rh}$  denote the resonant frequencies of the mixture, pure water and pure honey, respectively. The resonant frequencies measured and predicted by Equation (8) are compared in Table 5, where errors less than 0.5 % are found. Hence, the law of mixture can provide a useful guess about the resonance frequency change.

When more water is added, the quality factor is decreased first and then increased when  $\zeta$  is larger than 40 %. As shown in Figure 9, a third-order polynomial equation is adopted for curve fitting:

$$Q_U = 18036078.09 f_r^3 - 132313072.75 f_r^2 + 323541422.68 f_r - 263707964.13 \quad (9)$$

With a high coefficient of determination ( $R^2=0.99$ ), good correlation between the resonance frequency and quality factor is established.

Figure 8 Resonant responses of the water-adulterated honey samples

Table 4 Resonant parameters of the adulterated honey cases

Added water content $\zeta$ (%)	10	20	30	40	50
$f_r$ (GHz)	2.4695	2.4667	2.4616	2.4530	2.4503
$Q_U$	189.55	132.78	107.20	99.09	113.90

Table 5 Resonance frequencies predicted by Equation (8) and the corresponding errors

$\zeta$ (%)	10	20	30	40	50
$f_{rm}$ (GHz)	2.4711	2.4674	2.4637	2.4600	2.4562
Error (%)	0.06	0.03	0.08	0.28	0.24

Figure 9 Variation of the quality factor with respect to the resonant frequency for the honey-water mixtures

The permittivity of each adulteration case is presented in Figure 10.  $\varepsilon'_r$  of the mixture increases with increasing  $\zeta$  value, and a linear trend is shown. From the regression analysis, a linear relationship is obtained with  $R^2=0.98$ :

$$\varepsilon'_r = 96.51\zeta + 9.18 \quad (10)$$

Hence, the added water content can also be estimated by comparing the permittivity with that of pure honey. Considering the permittivity measurement uncertainty (around 5 % as shown in Table 3), the minimum added water content of approximately 0.5 % can be identified. In contrast to the quality factor,  $\varepsilon''_r$  increases as  $\zeta$  increases up to 40 % and then decreases. From the  $\varepsilon'_r - \varepsilon''_r$  plot given in Figure 11, a similar parabolic pattern is found ( $R^2=0.97$ ):

$$\varepsilon''_r = -0.01\varepsilon'^2_r + 1.14\varepsilon'_r - 5.26 \quad (11)$$

In Figure 10, the solid line denotes the pure honey case, and the dashed line denotes the value of pure water. It is indicated that  $\epsilon'_r$  of the mixture is between the two limits set by the water and honey, while  $\epsilon''_r$  is above both lines. Hence, the imaginary part is not subject to the law of mixture. The abnormality of  $\epsilon''_r$  is also seen in the literature (Guo et al., 2010; Puranik et al., 1991). It was suggested that some bound ions in the honey were released when water was added into honey (Puranik et al., 1991). In that case, ionic conduction also contributes to the dielectric polarisation of the mixture.

\*

Figure 10 Effect of the added water content on the permittivity of the honey-water mixture: (a)  $\epsilon'_r$ ;  
(b)  $\epsilon''_r$

Figure 11  $\epsilon'_r - \epsilon''_r$  relationship for the honey-water mixtures with varied  $\zeta$  values

### 3.5 Discussions

(1) The performance of the cavity for honey-water mixtures with very lower  $\zeta$  values, 2-8 % with an interval of 2 %, is further studied. The results are compared with the predictions using the relations found in the cases of higher  $\zeta$  values, i.e., Equations (8-11) are used for the predictions of the resonance frequency, quality factor,  $\epsilon'_r$  and  $\epsilon''_r$ , respectively. As seen in Table 6, the resonance frequency can be accurately predicted by the mixing law, and  $\epsilon'_r$  can be determined with an uncertainty below 5 %. Relatively higher discrepancies are shown in  $\epsilon''_r$  (errors below 10 %) and the quality factor (errors of 10-25 %). Hence, among the four parameters, the resonance frequency can be chosen as a more reliable indicator of the added water.

Table 6 Comparison between the measurement and prediction for the cases of  $\zeta=2-8$  %

$\zeta$ (%)	Parameters	Measurement	Prediction	Prediction error (%)
2	$f_r$ (GHz)	2.4742	2.4740	-0.01
	$Q_U$	301.02	333.64	10.84
	$\epsilon'_r$	11.28	11.11	-1.51
	$\epsilon''_r$	6.71	6.33	-5.71
4	$f_r$ (GHz)	2.4732	2.4733	0.01
	$Q_U$	242.73	299.10	23.22

	$\varepsilon_r'$	13.18	13.04	-1.06
	$\varepsilon_r''$	8.79	8.03	-8.67
	$f_r$ (GHz)	2.4722	2.4725	0.01
	$Q_U$	225.66	267.57	18.57
6	$\varepsilon_r'$	15.09	14.97	-0.79
	$\varepsilon_r''$	9.35	9.66	3.37
	$f_r$ (GHz)	2.4714	2.4718	0.02
	$Q_U$	196.54	243.07	23.68
8	$\varepsilon_r'$	16.71	16.90	1.14
	$\varepsilon_r''$	10.90	11.00	0.89

(2) The characteristic depth of penetration  $d_p$  is commonly used to describe the extent that an electromagnetic signal is attenuated within a medium. It is defined as the depth where the signal magnitude is reduced to  $1/e$  (about 37 %) of its original value and can be calculated by:

$$d_p = \frac{c}{\sqrt{2\pi f} \left\{ \varepsilon_r' \left[ \sqrt{1 + \left( \frac{\varepsilon_r''}{\varepsilon_r'} \right)^2} - 1 \right] \right\}^{1/2}} \quad (12)$$

The penetration depths for all the cases discussed are listed in Table 7. The ratio of the radius of the test sample  $r_1$  to  $d_p$ , represented by  $\kappa$ , is computed as well. With a  $\kappa$  value well below 5 %, it is revealed that the whole volume of the liquid sample can be fully interrogated by the microwave sensor.

Table 7 Penetration of the signal in all the cases investigated

	Water	Honey	Mixture ( $\zeta=2$ %)	Mixture ( $\zeta=4$ %)	Mixture ( $\zeta=6$ %)	Mixture ( $\zeta=8$ %)	Mixture ( $\zeta=10$ %)	Mixture ( $\zeta=20$ %)	Mixture ( $\zeta=30$ %)	Mixture ( $\zeta=40$ %)	Mixture ( $\zeta=50$ %)
$d_p$ (mm)	37.28	22.99	20.08	16.72	16.73	15.17	15.78	12.22	11.38	12.52	15.09
$\kappa$ (%)	1.34	2.17	2.49	2.99	2.99	3.30	3.17	4.09	4.39	3.99	3.31

#### 4 Concluding remarks

Here a new microwave approach has been presented for the detection of honey adulteration using the resonant responses of a  $TM_{010}$  mode cylindrical cavity resonator. In addition, the dielectric properties of the liquid sample under test can be computed from the changes in the resonance frequency and quality factor. Electromagnetic simulation has been carried out to reveal the resonant fields, from which the resonant frequency and optimal location for the sample displacement are verified.

From the measurement of distilled water, ethanol, IPA and 0.1M NaCl solution, it has been demonstrated that the permittivity values provided agree well with the empirical data. Specifically, for pure water, the error of the real part is approximately 5 %, while for the imaginary part a considerably lower error (within 1 %) is obtained.

For the Acacia honey and water-adulterated honey samples, it has been found that the variation of the resonance frequency with respect to the added water content conforms to the law of mixture. For the accurate measurement of the resonant frequency, the added water content can be readily determined. From the permittivity point of view, water is a dipolar molecule and has a high permittivity value. However, under the same temperature and frequency  $\epsilon'_r$  of the honey is much lower. When water is mixed with honey, the real part of the effective permittivity increases with increasing added water content in a monotonic pattern, and a linear relationship with high reliability of approximation has been established between the two parameters. In addition, there is a quadratic relationship between  $\epsilon'_r$  and  $\epsilon''_r$ . Hence, any added water in honey can also be detected from the permittivity measurement, and the water content related could be estimated. The abnormally high value of the imaginary part has been explained as a result of the changes in the dielectric polarisation. In the discussion of the signal penetration, it has been indicated that volumetric measurement can be offered.

Considering the simple test arrangement of the microwave sensor developed, it is envisaged that the sensor can be applied in a production line for online quality check of liquids. For practical applications custom-designed microwave circuits with a shorter frequency bandwidth can be employed to reduce the cost of the whole measurement system.

## Acknowledgement

This work was financially supported by the Natural Science Foundation of Jiangsu Province (Grant No. SBK2020044527), the Shuangchuang Project of Jiangsu Province (Grant No. KFR20020) and the Fundamental Research Funds for the Central Universities (Grant No. NS2020019). The first author gratefully acknowledges Dr.Fei Fei, Wei Wang (Keysight China) and Wenqing Xie (A-info Inc) for the assistance in the experiments.

## References:

- Agilent Technologies. (2006). *Agilent 85070E Dielectric Probe Kit 200 MHz to 50 GHz - Technical Overview. Measurement*. Santa Clara, CA, USA.
- Bázár, G., Romvári, R., Szabó, A., Somogyi, T., Éles, V., & Tsenkova, R. (2016). NIR detection of

honey adulteration reveals differences in water spectral pattern. *Food Chemistry*, 194, 873–880.  
<https://doi.org/10.1016/j.foodchem.2015.08.092>

Blakey, R. T., & Morales-Partera, A. M. (2016). Microwave dielectric spectroscopy – A versatile methodology for online, non-destructive food analysis, monitoring and process control. *Engineering in Agriculture, Environment and Food*, 9(3), 264–273.  
<https://doi.org/10.1016/j.eaef.2016.02.001>

Blasco, C., Fernández, M., Picó, Y., & Font, G. (2004). Comparison of solid-phase microextraction and stir bar sorptive extraction for determining six organophosphorus insecticides in honey by liquid chromatography–mass spectrometry. *Journal of Chromatography A*, 1030(1–2), 77–85.  
<https://doi.org/10.1016/j.chroma.2003.11.037>

Chen, L. F., Ong, C. K., Neo, C. P., Varadan, V. V., & Varadan, V. K. (2004). *Microwave Electronics: Measurement and Materials Characterization*. Chichester, UK: John Wiley & Sons, Ltd. Retrieved from <http://doi.wiley.com/10.1002/0470020466>

Chen, L., Xue, X., Ye, Z., Zhou, J., Chen, F., & Zhao, J. (2011). Determination of Chinese honey adulterated with high fructose corn syrup by near infrared spectroscopy. *Food Chemistry*, 128(4), 1110–1114. <https://doi.org/10.1016/j.foodchem.2010.10.027>

Cole, K. S., & Cole, R. H. (1941). Dispersion and Absorption in Dielectrics I. Alternating Current Characteristics. *The Journal of Chemical Physics*, 9(4), 341–351.  
<https://doi.org/10.1063/1.1750906>

Collin, R. E. (2000). *Foundations for Microwave Engineering* (2nd ed.). Wiley-IEEE Press.

Gennarelli, G., Romeo, S., Scarfi, M. R., & Soldovieri, F. (2013). A Microwave Resonant Sensor for Concentration Measurements of Liquid Solutions. *IEEE Sensors Journal*, 13(5), 1857–1864.  
<https://doi.org/10.1109/JSEN.2013.2244035>

Gibson, A. A. P., Ng, S. K., Noh, B. B. M., Chua, H. S., Haigh, A. D., Parkinson, G., ... Plunkett, A. (2008). An overview of microwave techniques for the efficient measurement of food materials. *Food Manufacturing Efficiency*, 2(1), 35–43. <https://doi.org/10.1616/1750-2683.0026>

Gregory, A. P., & Clarke, R. N. (2012). *Tables of the complex permittivity of dielectric reference liquids at frequencies up to 5 GHz*.

Guo, W., Zhu, X., Liu, Y., & Zhuang, H. (2010). Sugar and water contents of honey with dielectric property sensing. *Journal of Food Engineering*, 97(2), 275–281.  
<https://doi.org/10.1016/j.jfoodeng.2009.10.024>

Hammel, Y.-A., Mohamed, R., Gremaud, E., LeBreton, M.-H., & Guy, P. A. (2008). Multi-screening approach to monitor and quantify 42 antibiotic residues in honey by liquid chromatography–tandem mass spectrometry. *Journal of Chromatography A*, 1177(1), 58–76.



<https://doi.org/10.1016/j.chroma.2007.10.112>

- Hippel, A. R. Von. (1995). *Dielectric materials and applications* (2nd ed.). New York: Artech House. Retrieved from <http://cds.cern.ch/record/270934>
- Krupka, J. (2006). Frequency domain complex permittivity measurements at microwave frequencies. *Measurement Science and Technology*, 17(6), R55–R70. <https://doi.org/10.1088/0957-0233/17/6/R01>
- Li, Z., Haigh, A., Soutis, C., Gibson, A., & Sloan, R. (2017). Evaluation of water content in honey using microwave transmission line technique. *Journal of Food Engineering*, 215, 113–125. <https://doi.org/10.1016/j.jfoodeng.2017.07.009>
- Pozar, D. M. (2012). *Microwave Engineering*. John Wiley & Sons, Inc. (Fourth edi). New York: John Wiley & Sons. <https://doi.org/10.1007/s13398-014-0173-7.2>
- Puranik, S., Kumbharkhane, A., & Mehrotra, S. (1991). Dielectric properties of honey-water mixtures between 10 MHz to 10 GHz using time domain technique. *Journal of Microwave Power and Electromagnetic Energy*, 26(4), 196–201. <https://doi.org/10.1080/08327823.1991.11688157>
- Regier, M., Knoerzer, K., & Schubert, H. (2017). *The Microwave Processing of Foods*. Elsevier. <https://doi.org/10.1016/C2014-0-04182-2>
- Stogryn, A. (1971). Equations for Calculating the Dielectric Constant of Saline Water (Correspondence). *IEEE Transactions on Microwave Theory and Techniques*, 19(8), 733–736. <https://doi.org/10.1109/TMTT.1971.1127617>
- Wang, S., Guo, Q., Wang, L., Lin, L., Shi, H., Cao, H., & Cao, B. (2015). Detection of honey adulteration with starch syrup by high performance liquid chromatography. *Food Chemistry*, 172, 669–674. <https://doi.org/10.1016/j.foodchem.2014.09.044>
- Zábrodská, B., & Vorlová, L. (2014). Adulteration of honey and available methods for detection – a review. *Acta Veterinaria Brno*, 83(10), S85–S102. <https://doi.org/10.2754/avb201483S10S85>